Reactive Neural Control for Phototaxis and Obstacle Avoidance Behavior of Walking Machines

Poramate Manoonpong, Frank Pasemann, and Florentin Wörgötter

***Abstract*—This paper describes reactive neural control used to generate phototaxis and obstacle avoidance behavior of walking machines. It utilizes discrete-time neurodynamics and consists of two main neural modules: neural preprocessing and modular neural control. The neural preprocessing network acts as a sensory fusion unit. It filters sensory noise and shapes sensory data to drive the corresponding reactive behavior. On the other hand, modular neural control based on a central pattern generator is applied for locomotion of walking machines. It coordinates leg movements and can generate omnidirectional walking. As a result, through a sensorimotor loop this reactive neural controller enables the machines to explore a dynamic environment by avoiding obstacles, turn toward a light source, and then stop near to it.**

***Keywords*—Recurrent neural networks, Walking robots, Modular neural control, Phototaxis, Obstacle avoidance behavior.**

I. Introduction

RECOGNIZING that, to date, most research in the domain of biologically inspired walking machines concentrated on the construction of machines with animal-like properties performing efficient locomotion [1], [2]. Others have focused on the generation of locomotion based on engineering technologies [3] as well as biological principles [4], [5]. In general, all these machines were solely designed for the purpose of motion without responding to environmental stimuli. In this research area, only a few of them have attended to implement different (reactive) behaviors on physical walking machines [3], [6]. This highlights that less attention has been paid to the walking machines which can react to environmental stimuli. In other words, contributions developing embodied control techniques for various reactive behaviors of many degrees-of-freedom systems are rare.

From this point of view, in this article, we present a physical walking machine which can interact with a dynamic environment by performing obstacle avoidance and phototaxis. That is the walking machine can explore its environment by avoiding obstacles (negative tropism), turn toward a light source (positive tropism), and then stop near to it. These desired behaviors are inspired by the first autonomous two-drive-wheel robots $Elmer$ and $Elsie$ of Grey Walter [7] which were also capable of responding to a light stimulus and avoiding obstacles. To this end, we are able to reproduce such reactive behaviors, generally achieved for the wheeled robots, for a machine with many degrees of freedom facing sensorimotor coordination problems of a more complex system. However, the main purpose of this article is not only to demonstrate the walking machine performing different types of tropism but also to investigate the analyzable neural mechanisms underlying this approach in order to understand their inherent dynamical properties. Furthermore, in this study, we will try to show that reactive neural control can be a powerful technique to better understand and solve sensorimotor coordination problems of many degrees-of-freedom systems like sensor-driven walking machines.

The following section describes the technical specifications of the walking machine. Section 3 explains a reactive neural controller for phototaxis and obstacle avoidance behavior. The experiments and results are discussed in section 4. Conclusions are given in the last section.

Manuscript received September 18, 2007. This work was supported in part by the German Research Foundation (Deutsche Forschungsgemeinschaft DFG).

Poramate Manoonpong is with Bernstein Center for Computational Neuroscience, University of Göttingen, Göttingen D-37073, Germany (corresponding author to provide phone: +49(0)5515176-530; fax: +49(0)5515176-449; e-mail: poramate@bccn-goettingen.de).

Frank Pasemann is with Fraunhofer-Institut für Intelligente Analyse- und Informationssysteme (IAIS), Sankt Augustin D-53754, Germany (e-mail: frank.pasemann@iais.fraunhofer.de).

Florentin Wörgötter is with Bernstein Center for Computational Neuroscience, University of Göttingen, Göttingen D-37073, Germany (e-mail: worgott@bccn-goettingen.de).

II. The Walking Machine AMOS-WD06

The AMOS-WD06 [8] is a hexapod robot. Each leg has three joints (three DOF): the thoraco-coxal (TC-) joint enables forward (+) and backward (−) movements, the coxa-trochanteral (CTr-) joint enables elevation (+) and depression (−) of the leg, and the femurtibia (FTi-) joint enables extension (+) and flexion (−) of the tibia (see Fig. 1b). Each tibia segment has a spring damped compliant element to absorb impact force as well as to measure ground contact during walking. All leg joints are driven by analog servo motors. The machine is constructed with two body parts: a front part where two forelegs are installed and a central body part where two middle legs and two hind legs are attached. They are connected by one active backbone joint driven by a digital servo motor. This machine has six foot contact sensors, seven infrared (IR) sensors, two light dependent resistor (LDR) sensors, and one upside-down detector (UD) sensor (see Fig. 1a). The foot contact sensors are for recording and analyzing the walking patterns. The IR sensors are used to elicit negative tropism, e.g., obstacle avoidance and escape response, while the LDR sensors serve to activate positive tropism like phototaxis. The UD sensor is applied to trigger a self-protective reflex behavior when the machine is turned into an upside-down position (see [9] for details).

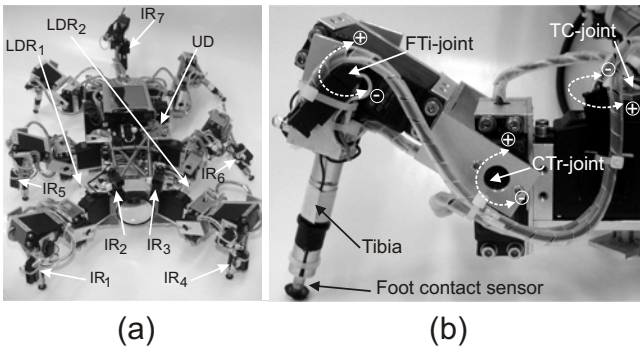

Fig. 1. (a) The physical six-legged walking machine AMOS-WD06. (b) The physical leg with three DOF of the AMOS-WD06

III. Reactive Neural Control

Reactive neural control (see Fig. 2) for phototaxis (positive tropism) and obstacle avoidance (negative tropism) behavior is formed by two main modules: the neural preprocessing unit and the modular neural control unit. The neural preprocessing unit serves also for sensory fusion. It filters sensory noise and shapes sensory data to drive the corresponding reactive behavior. The modular neural control unit is used for locomotion generation of the walking machine. It coordinates leg movements and can generate omnidirectional walking. The details of these two neural units are described in the following sections.

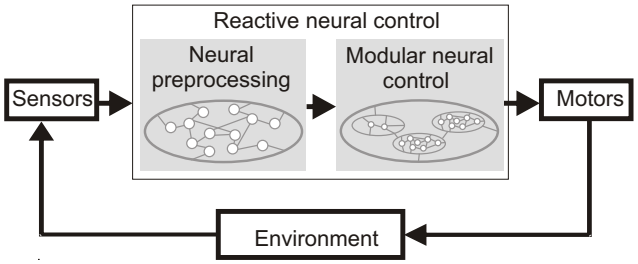

Fig. 2. Diagram of reactive neural control. The controller acts as an artificial perception-action system, i.e., the sensor signals go through the neural preprocessing into the modular neural control which commands the actuators. As a result, the robot's behavior is generated by interacting with its environment in a sensorimotor loop

All neurons of the network are modeled as discrete-time non-spiking neurons. The activation and output of each neuron are governed by (1), (2), respectively:

$$a_i(t+1) = \sum_{j=1}^{n} W_{ij}\, o_j(t) + B_i \quad i = 1, \ldots, n, \quad (1)$$

$$o_i = \tanh(a_i), \quad (2)$$

where n denotes the number of units, a_i their activity, B_i represents a fixed internal bias term together with a stationary input of neuron i, W_{ij} the synaptic strength of the connection from neuron j to neuron i, and o_i the output of neuron i. Input units, e.g., sensory neurons, are configured as linear buffers.

A. Neural Preprocessing of Sensory Data

In order to generate the reactive phototaxis and obstacle avoidance behavior representing as orientational responses, we make use of two LDR ($LDR_{1,2}$, positive stimuli) and only four front IR ($IR_{1,\ldots,4}$, negative stimuli) sensor signals (see Fig. 7). These sensory data provide environmental information for our sensor-driven robot system. Nonetheless, the raw sensory signals require preprocessors to eliminate the sensory noise as well as to shape all sensory data for activating the appropriate reactive behavior. To do so, neural preprocessing is applied. It is constructed based on the minimal recurrent controller (MRC) structure [10]. The original controller [10] (colored box in Fig. 3) has been developed for controlling only obstacle avoidance behavior of a miniature Khepera robot, which is a two wheeled platform. Here, it is adjusted and expanded for controlling the walking behavior of the machine to avoid obstacles or escape from a deadlock situation (negative tropism) as well as turn toward and approach a light source (positive tropism).

The principle connection weights $W_{1,\ldots,4}$ of the network were manually adjusted with respect to dynamical properties of recurrent neural networks as follows. First, the self-connection weights $W_{1,2}$ of the output neurons $O_{1,2}$ were manually tuned to derive a reasonable hysteresis interval on the input space. That is the width of the hysteresis is proportional to the strength of the self-connections (see [8], [9] for details). In this case, the hysteresis effect determines the turning angle for avoiding obstacles and approaching a light source, i.e., the wider the hysteresis, the larger the turning angle. Both self-connections are set to 2.0 to obtain a suitable turning angle of the AMOS-WD06 (see Figs. 4a and c). Then, the recurrent connections $W_{3,4}$ between output neurons were symmetrized and manually adjusted to -3.5. Such inhibitory recurrent connections are formed as a so-called even loop [11], which also shows hysteresis phenomenon (see Fig. 4b). In general conditions, only one neuron at a time is able to produce a positive output, while the other one has a negative output, and vice versa. However, both neurons can show high activation only if their inputs are very high, e.g., > 0.64 (see Fig. 4b). This guarantees the optimal functionality for avoiding obstacles or escaping from corner and deadlock situations.

The sensor values ($LDR_{1,2}$ and $IR_{1,\ldots,4}$) are linearly mapped into the closed interval $[-\mathbf{1}, +\mathbf{1}]$. For the LDR sensors, values $LDR_{1,2} = -1.0$ refers to darkness and $LDR_{1,2} = +1.0$ to the maximal measurable light intensity. The IR values $IR_{1,\ldots,4}$ are -1.0 if no obstacle is detected and value $+1.0$ represents that an obstacle is near. The mean value of the two left IR sensor signals ($IR_{3,4}$) is used as the first input ($Input1$) to the network while the second input ($Input2$) corresponds to the two right IR sensors ($IR_{1,2}$). Parallelly, the left and right LDR sensor signals are provided as the third ($Input3$) and forth ($Input4$) inputs indirectly passing through hidden neurons $H_{1,2}$. Concerning the priority of the sensory signals, here the IR sensor signals are desired to have higher priority than the LDR sensor signals. That is if obstacles and light are detected at the same time, the neural preprocessor has to elicit IR sensor signals and inhibit LDR sensor signals. As a

consequence, the obstacle avoidance behavior will be executed instead of the phototaxis. The phototaxis is performed if and only if the obstacles are not detected. To do so, we set the connection weights $W_{5,6}$ from $Input1$ and $Input2$ to the output units to higher values than the ones $W_{7,8}$ connecting between the hidden and output neurons. Thus, they were set to $W_{5,6} = 7.0$ and $W_{7,8} = 4.5$. To ensure the optimal functionality for priority setting of the sensory signals, we additionally project two inhibitory connections $W_{9,10}$ from $Input1$ and $Input2$ to H_1 and H_2, respectively, together with a bias term B at each of the hidden neuron. These parameters were again manually tuned and were, as a result, set to $W_{9,10} = -2.0$ and $B_{1,2} = -1.5$. Furthermore, two inhibitory synapses $W_{11,12}$ were extra integrated and set with the same strength of $W_{7,8}$, i.e., -4.5. These inhibitory cross connections cause that an activated output neuron (showing high activation $\approx +1$) driven by its ipsilateral LDR signal can become deactivated (showing low activation ≈ -1) if the contralateral LDR signal becomes activated (see Fig. 4d). An important effect of this cross inhibition is to obtain effective phototaxis; i.e., the machine is able to walk forward during performing phototaxis and finally can approach to the source. On the other hand, without these cross inhibition the machine will only try to turn toward the source without performing forwards motion. As a consequence, such a behavior might have difficulties to approach the source.

Note that one can optimize the network parameters, for instance by using an evolutionary algorithm [10], [12] but for our purposes here, it is good enough. The complete preprocessing network and its hysteresis effect are shown in Figs. 3 and 4, respectively.

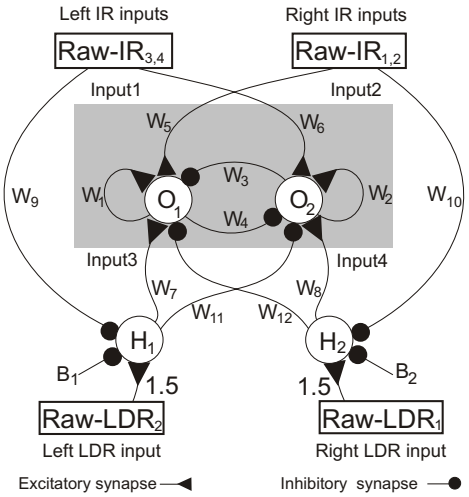

Fig. 3. The neural preprocessing network for the coordination of positive (LDR sensor signals) and negative (IR sensor signals) stimuli. Its outputs $O_{1,2}$ are directly fed to input neurons $I_{4,5}$ of the modular neural control (see Fig. 5) to stimulate the phototaxis and obstacle avoidance behavior of the AMOS-WD06. Note that $H_{1,2}$ are the hidden neurons of the network

This structure and its parameters cause the network to filter, prioritize, and coordinate the different sensory inputs. It can even determine the turning angle as well as the turning direction of the walking machine by utilizing the hysteresis

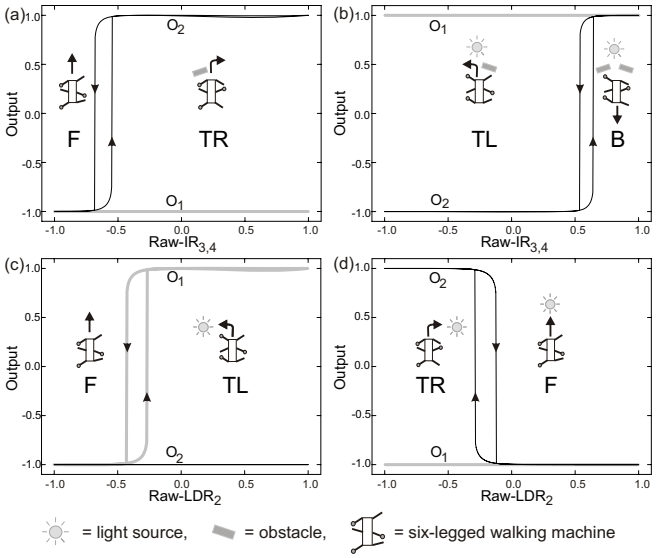

Fig. 4. (a), (b) Hysteresis domain of $Input1$ ($Raw - IR_{3,4}$) for the output neuron O_2 of the network while the other output neuron O_1 shows low ≈ -1 and high $\approx +1$ activation, respectively. All other sensory inputs ($Raw - IR_{1,2}$, $Raw - LDR_1$, and $Raw - LDR_2$) are fixed to ≈ -1 for case (a) but $\approx +1$ for case (b). In case (a), the machine will walk forward $\mathbf{F}$ (drawing on the left) as long as O_1 and O_2 give low activation but it will turn right $\mathbf{TR}$ as soon as $Raw - IR_{3,4}$ increases to values above -0.55 where only O_2 shows high activation meaning that there is an obstacle on its left (drawing on the right). However, it will return to walk forward $\mathbf{F}$ when $Raw - IR_{3,4}$ decreases to values below -0.68 meaning that no obstacle is detected. In case (b), the machine will turn left $\mathbf{TL}$ (i.e., it avoids an obstacle on its right although it detects a light source in front of it, compare drawing on the left) as long as the value of $Raw - IR_{3,4}$ is below 0.64 where O_1 has high activation while O_2 shows low activation. Increasing the value of $Raw - IR_{3,4}$ above 0.64 causes O_2 to become active. The machine then walks backward $\mathbf{B}$, i.e., it detects obstacles on both sides (drawing on the right). It will return to turn left $\mathbf{TL}$ again if the value of $Raw - IR_{3,4}$ is below 0.54. (c) Hysteresis domain of $Input3$ (corresponding to $Raw - LDR_2$) for O_1 with the other inputs fixed to ≈ -1. O_1 shows high activation if $Raw - LDR_2$ increases to values above -0.25 and returns to low activation if $Raw - LDR_2$ decreases to values below -0.4 while O_2 shows low activation in all cases. As a result, the machine will turn left $\mathbf{TL}$ (drawing on the right) when O_1 shows high activation meaning that it turns toward a light source otherwise it walks forward (drawing on the left). (d) Hysteresis domain of $Raw - LDR_2$ for O_2 with the other inputs fixed as $Raw - IR_{1,2,3,4} \approx -1$ and $Raw - LDR_1 \approx +1$. Here, O_2 shows low activation only if the value of $Raw - LDR_2$ is higher than -0.13 while O_1 gives low activation all the time. However, O_2 will provide high activation if $Raw - LDR_2$ decreases to values below -0.28. As a consequence, the machine will turns toward the source (drawing on the left) and then it is able to walk forward if the source is almost in front of it (drawing on the right) causing high activation of both LDR signals ($Raw - LDR_{1,2}$). Finally, it can approach to the source. In reverse cases, if $Raw - IR_{1,2}$ and $Raw - LDR_1$ are varied while the other inputs are fixed, they will derive the same hysteresis effect as $Raw - IR_{3,4}$ and $Raw - LDR_2$ do

effect. Applying the output signal of O_1 and O_2 (see Fig. 7) to their target neurons I_4 and I_5 in the neural control module (see Fig. 5), the walking machine can autonomously perform phototaxis and obstacle avoidance behavior through a sensori-motor loop with respect to environmental stimuli. In other words, the walking machine will turn toward, approach, and eventually stop near a light source by determining a threshold of the mean value of the left and right LDR sensor signals ($MLDR$). At the same time, it will also avoid obstacles if they are detected.

B. Modular Neural Control

Modular neural control for locomotion of the walking machine consists of three subordinate networks[1] or modules (colored boxes in Fig. 5): a neural oscillator network, two velocity regulating networks (VRNs), and a phase switching network (PSN). The neural oscillator network, serving as a central pattern generator (CPG) [13], generates periodic output signals. These signals are provided to all CTr-joints and FTi-joints only indirectly passing through all hidden neurons of the PSN. TC-joints are regulated via the VRNs. Thus, the basic rhythmic leg movement is generated by the neural oscillator network and the steering capability of the walking machine is realized by the PSN and the VRNs. Fig. 5 shows the complete network structure together with the synaptic weights of the connections between the controller and the corresponding motor neurons as well as the bias term of each motor neuron. These synaptic weights and all bias terms were manually adjusted to obtain an optimal gait; i.e., a typical tripod gait where the diagonal legs are paired and move synchronously.

This modular neural control can generate different walking patterns which are controlled by the four input neurons $I_{2,\ldots,5}$. Furthermore, a self-protective reflex[2] can be activated via the input neuron I_1 which will excite TR_1 and TL_1 joints and all CTr- and FTi- joints and inhibit the remaining TC-joints. Appropriate input parameter sets for the different walking patterns and the reflex behavior are presented in Table I where the first column describes the desired actions in accordance with five input parameters shown in the other columns. Abbreviations are: $FDiR$ and $BDiR$ = forward and backward diagonal motion to the right, $FDiL$ and $BDiL$ = forward and backward diagonal motion to the left, LaR and LaL = lateral motion to the right and the left. Note that marching is an action where all the legs are positioned and held in a vertical position and support is switched between the two tripods.

TABLE I
INPUT PARAMETERS FOR THE DIFFERENT WALKING PATTERNS AND THE REFLEX BEHAVIOR

Actions	I_1	I_2	I_3	I_4	I_5
Forward	0	1.0	1, 0	-1.0	-1.0
Backward	0	1.0	1, 0	1.0	1.0
Turn right	0	1.0	1, 0	-1.0	1.0
Turn left	0	1.0	1, 0	1.0	-1.0
Marching	0	1.0	1, 0	0.0	0.0
FDiR	0	0.0	0	-1.0	-1.0
BDiR	0	0.0	0	1.0	1.0
LaR	0	0.0	0	0.0	0.0
FDiL	0	0.0	1	-1.0	-1.0
BDiL	0	0.0	1	1.0	1.0
LaL	0	0.0	1	0.0	0.0
Reflex	1	0.0 ...1.0	1, 0	-1.0 ...1.0	-1.0 ...1.0

As shown in Table I, this neural controller can produce at least 12 different actions with respect to the given inputs.

[1]Here, we discuss only main functions of the network. A more complete description of each subordinate network is given in [8], [9].

[2]The action is triggered when the machine is turned into an upside-down position. As a consequence, it stands still in this position as long as the stimulus (UD signal) is presented (not shown here but see [9] for details).

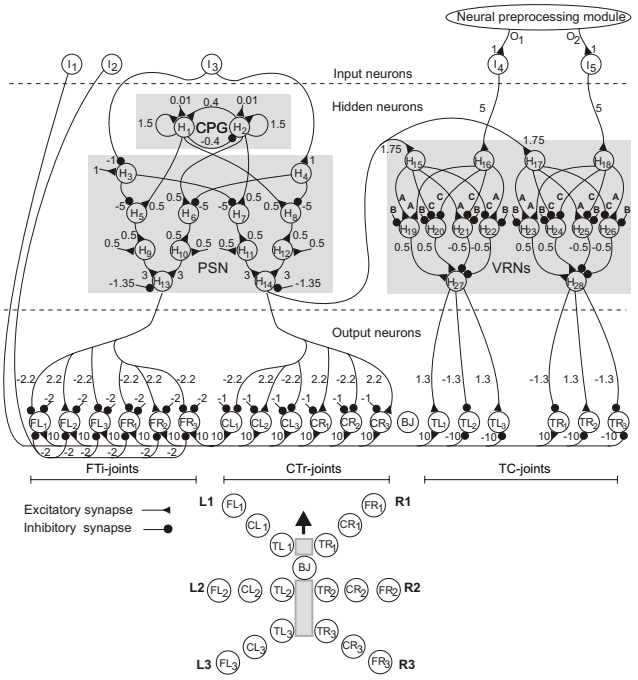

Fig. 5. The modular neural control of the six-legged walking machine AMOS-WD06 consists of three different neuron groups: input, hidden, and output. Input neurons I are the neurons used to control walking direction ($I_{2,\ldots,5}$) and to trigger the protection reflex (I_1). Hidden neurons H are divided into three modules (CPG, VRNs, and PSN (see [8], [9] for details)). Output neurons (TR, TL, CR, CL, FR, FL) directly command the position of servo motors. Abbreviations are: BJ = a backbone joint, TR(L) = TC-joints of right (left) legs, CR(L) = CTr-joints of right (left) legs, FR(L) = FTi-joints of right (left) legs. All connection strengths together with bias terms are indicated by the small numbers except some parameters of the VRNs given by A = 1.7246, B = -2.48285, C = -1.7246. The location of the motor neurons on the AMOS-WD06 is shown in the lower picture. Note that describing the controller driving the machine also with the backbone joint will go beyond the scope of this article. Thus, the motor neuron controlling the backbone joint BJ is not activated; i.e., the backbone joint functions as a rigid connection. However, it can be modulated by the periodic signal via the PSN or VRNs to perform an appropriate motion, e.g., helping the machine during climbing over obstacles or performing other tasks

For all cases, I_1 and I_3 are set as binary values (0 or 1) which then activate or inhibit the movement of all joints and control directions of diagonal or lateral walking, respectively. On the other hand, I_2 can vary between 0.0 and 1.0 which suppresses the amplitude of the periodic signal of the FTi-joints; i.e., the larger the value of I_2 the lower the amplitude. As a consequence, the walking machine will perform a very small step in the lateral or diagonal direction or no step at all if I_2 is set to 1.0. Setting I_2 to negative values might cause unstable walking.

Furthermore, varying I_4 and I_5 between -1.0 and 1.0 (see Fig. 6) while other input parameters are fixed (I_1 = 0, I_2 = 1.0, and I_3 = 1 or 0), the amplitude of the periodic signals of the left and right TC-joints will be regulated. As a consequence, the machine can perform straight and curve walking in forward and backward directions, marching, and spot turning in different radians (orientational motions). According to these parameter settings, it is appropriate and simple to generate the phototaxis and obstacle avoidance behavior

because such behavior corresponds mainly to orientational motions rather than diagonal or lateral motions. Thus, in the robot walking experiments presented in the following section, the input parameters $I_{1,\ldots,3}$ are fixed as described above where the diagonal and lateral motions as well as the reflex action are deactivated. On the other hand, $I_{4,5}$ will be stimulated by preprocessed sensory signals coming from the neural preprocessor (see Fig. 3). As a result, the walking machine will walk forward if no obstacle or light is detected and it will turn right or left with respect to the sensory signals, e.g., turn toward a light source (positive stimuli) but turn away from obstacles (negative stimuli). It will also perform marching as soon as it closely approaches a light source.

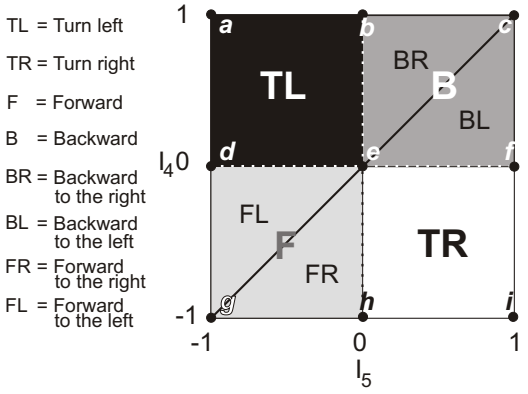

Fig. 6. Plot of the input space (I_4, I_5, see Fig. 5) which is classified into four main areas. For input values in a dark square area ($\overline{dabe}$), the walking machine will perform spot turning to the left with different radians while a white square area ($\overline{efih}$) is for the right turn. In light gray triangle areas ($\overline{gde}$ and $\overline{geh}$), they will move forward in different curves to the left and the right and dark gray triangle areas ($\overline{ebc}$ and $\overline{ecf}$) are for backward to the right and the left, respectively. Additionally, if I_4 and I_5 are varied along the diagonal line ($\overline{gec}$), the machines will walk straight forward ($\overline{ge}$) and backward ($\overline{ec}$) with different walking speeds. Details on robot walking experiments have been presented in [9]

IV. Experiments and Results

This section describes experiments carried out to assess the ability of the reactive neural controller to generate phototaxis and obstacle avoidance as well as exploration behaviors. The controller was implemented on a mobile processor (a PDA) for testing the physical walking machine in a real environment[3]. We encourage readers to watch the video clips of the real robot walking experiments at http://www.nld.ds.mpg.de/∼poramate/ICIS. Here, we report the real time data of sensory and motor signals of the walking machine during performing reactive behaviors in different situations (see Fig. 7). Recall that generating the reactive behaviors which correspond to orientation motions will effect only the movement of the TC-joints (compare TR_1 and TL_1 in Fig. 7) while the periodic movement of the CTr-joints will remain unchanged (compare CR_1 in Fig. 7) and the FTi-joints will be inhibited (compare FR_1 in Fig. 7). Note that in the experiments the machine walks with one gait type where the diagonal legs are paired and move together; e.g., R_1, R_3, and L_2 step in phase while the remaining legs step out of phase. Such that the motor signals of R_1, R_3, and L_2 have similar patterns and perform 180 degrees out of phase with other motor signals of L_1, R_2, and L_3.

[3]During experiments, we use battery packs for powering the robot system which can run up to 35 minutes.

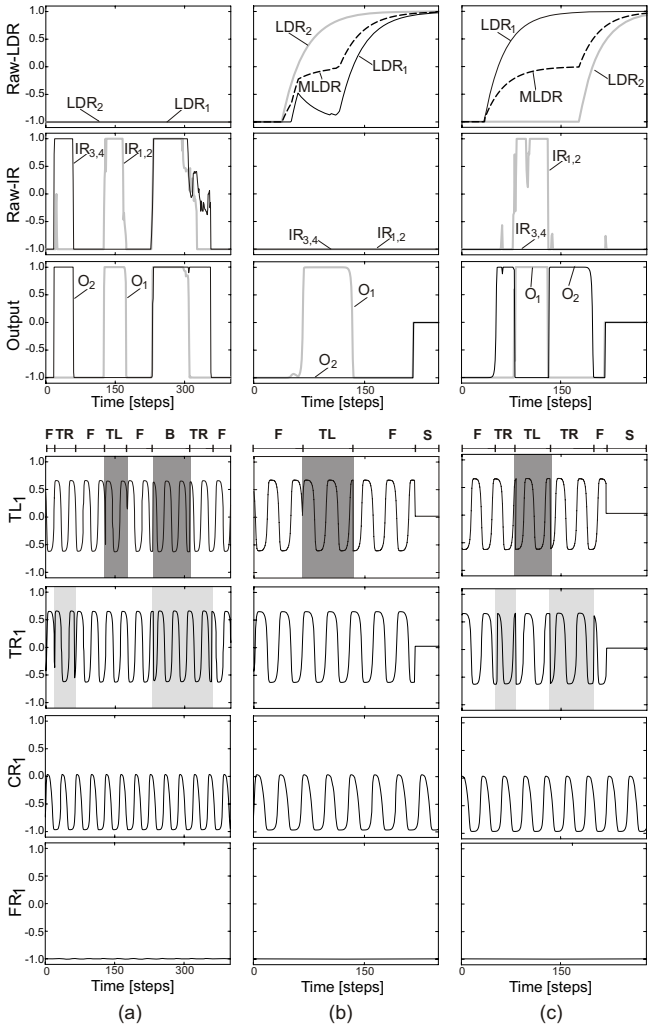

Fig. 7. Sensory and motor signals during performing the reactive behaviors. (a) Obstacle avoidance behavior. (b) Phototaxis. (c) Obstacle avoidance behavior and phototaxis (see text for details). Abbreviations are: $IR_{1,\ldots,4}$ = raw IR sensor signals; $LDR_{1,2}$ = raw LDR sensor signals; $MLDR$ = the mean value of the left and right LDR sensor signals; $O_{1,2}$ = outputs of the neural preprocessor (see Fig. 3); $\mathbf{F}$ = forward; $\mathbf{TL}$ = turn left; $\mathbf{TR}$ = turn right; $\mathbf{B}$ = backward; $\mathbf{S}$ = stop; TR_1, CR_1, FR_1 = motor signals of the TC-joint, CTr-joint, and FTi-joint of the right front leg, respectively; TL_1 = the motor signal of the TC-joint of the left front leg

Fig.7a shows the situation where the walking machine performed only obstacle avoidance behavior. It can be seen that TR_1 is turned into the opposite direction (light gray area), if the left IR sensors ($IR_{3,4}$) detects the obstacle; correspondingly TL_1 is turned into the opposite direction (dark gray area) when the right IR sensor signal ($IR_{1,2}$) is active. As a consequence, the walking machine was able to turn away from an obstacle and finally avoid it. In other words, it turned right $\mathbf{TR}$ if there was the obstacle on its left and vice versa otherwise it walked forward $\mathbf{F}$. In special

situations, e.g., here walking toward a wall, IR sensor signals on both sides were simultaneously active. Thus, TR_1 and TL_1 were reversed into another directions which causes the machine to walk backward **B**. During walking backward the right IR sensor signal became inactive while the left one was still active. As a result, the active signal drove the machine to turn right **TR** until; eventually, it was able to avoid the obstacle and then continued walking forward **F**.

Fig.7b presents the situation where the walking machine detected a light source and no obstacles appeared around it. It can be seen that TL_1 is turned into the opposite direction (dark gray area), if the left LDR sensor (LDR_2) detects the source. On the other hand, if the right LDR sensor signal (LDR_1) is active, TR_1 will be reversed (not shown). During turning toward the source, both LDR sensor signals got high activation the result of which enabled the machine to walk forward **F**. After that the walking machine approached the source and eventually stopped **S** nears it by marching if the amplitude of the mean value of the left and right LDR sensor signals $MLDR$ becomes larger than a threshold value (here, 0.94). This results in the motor signals of all TC-joints being automatically set to 0.0.

Fig. 7c demonstrates the situation where an obstacle was detected during performing phototaxis. At the beginning, the walking machine walked forward **F** where $O_{1,2}$ were inactive (≈ -1) and then turned toward the source as soon as one of the LDR signal shows high activation (here, LDR_1 meaning that the source was on its right). It turned right by inverting the signals of all right TC-joints (compare TR_1, light gray area). While turning toward the source, the machine detected the obstacle on its right where $IR_{1,2}$ became active. As a consequence, it turned left **TL** to avoid the obstacle (see the inversion of the motor signal of TL_1, dark gray area) although it still detected the source. After avoiding the obstacle it then again turned toward the source and finally stopped **S** in front of it.

As demonstrated, the reactive neural controller is suitable to successfully enable the machine to perform phototaxis and solve the obstacle avoidance task. Additionally, the controller can even protect the machines from getting stuck in corners or deadlock situations. This is demonstrated in a video clip at http://www.nld.ds.mpg.de/∼poramate/ICIS. Thus, due to this functionality, the walking machines can autonomously perform exploration.

V. Conclusion

The six-legged walking machine AMOS-WD06 is presented as a reasonably complex robot platform for studying sensorimotor coordination problems of many degrees-of-freedom systems, for conducting experiments with neural controllers, and even for testing artificial perception-action systems.

In this study the controller of the walking machine was designed purely as a neural network. It consists of two neural modules: neural preprocessing and modular neural control. The neural preprocessing unit obtained by a small recurrent neural network functions as a sensor fusion unit. Utilizing hysteresis phenomena of such a network, it can filter sensory noise and combine different sensory signals to stimulate the desired positive and negative tropisms of the walking machine. The modular neural control, on the other hand, performs as a locomotion generator. It was constructed by integrating three different functional neural modules: the neural oscillator network, the velocity regulating networks, and the phase switching network. The neural oscillator network acts as a CPG for basic rhythmic leg movements while controlling different walking patterns is done by the velocity regulating and the phase switching networks. This modular neural control can produce at least 11 different walking patterns and a self-protective reflex by using five input neurons. Coupling the neural preprocessing with the modular neural control leads to a so-called reactive neural control. It has been implemented on the embedded system (mobile processor) of the walking machine. As a result, the walking machine can autonomously perform different types of tropisms, like phototaxis and obstacle avoidance behavior using the sensorimotor loop. The proposed neural technique has been shown to be adequate for generating locomotion and various reactive behaviors of the walking machine. It can even easily be adapted to control different kinds of walking machines without changing the internal network structure and its parameters [9]. Furthermore, modifying the neural preprocessing or adding another preprocessing units another kind of a reactive behavior, e.g., sound tropism, [14] can be also obtained.

References

[1] S. Fujii and T. Nakamura, “Development of an amphibious hexapod robot based on a water strider,” in *Proc. 10th International Conference on Climbing and Walking Robots*, pp. 135-143, 2007.

[2] A. J. Ijspeert, A. Crespi, D. Ryczko, and J. M. Cabelguen, “From swimming to walking with a salamander robot driven by a spinal cord model,” *Science*, vol. 315, pp. 1416-1420, 2007.

[3] R. A. Brooks, “A robot that walks: emergent behaviors from a carefully evolved network,” *Neural Computation*, vol. 12, pp. 253-262, 1989.

[4] H. Cruse, T. Kindermann, M. Schumm, J. Dean, and J. Schmitz, “Walknet-A biologically inspired network to control six-legged walking,” *Neural Networks*, vol. 11, pp. 1435-1447, 1998.

[5] H. Kimura, Y. Fukuoka, and A. H. Cohen, “Adaptive dynamic walking of a quadruped robot on natural ground based on biological concepts,” *International Journal of Robotics Research*, vol. 26, pp. 475-490, 2007.

[6] R. C. Arkin, K. Ali, A. Weitzenfeld, and F. Cervantes-Perez, “Behavior models of the praying matis as a basis for robotic behavior,” *Robotics and Autonomous Systems*, vol. 32, pp. 39-60, 2000.

[7] W. G. Walter, *The Living Brain*, New York: Norton, 1953.

[8] P. Manoonpong, *Neural Preprocessing and Control of Reactive Walking Machines: Towards Versatile Artificial Perception-Action Systems*, Cognitive Technologies, Springer, 2007.

[9] P. Manoonpong, F. Pasemann, and F. Woergoetter, “Sensor-driven neural control for omnidirectional locomotion and versatile reactive behaviors of walking machines,” *Robotics and Autonomous Systems*, doi:10.1016/j.robot.2007.07.004, 2007, in press.

[10] F. Pasemann, M. Huelse, and K. Zahedi, “Evolved neurodynamics for robot control,” in *Proc. European Symposium on Artificial Neural Networks*, vol. 2, pp. 439-444, 2003.

[11] F. Pasemann, “Discrete dynamics of two neuron networks,” *Open Systems and Information Dynamics*, vol. 2, pp. 49-66, 1993.

[12] M. Huelse, S. Wischmann, and F. Pasemann, “The role of non-linearity for evolved multifunctional robot behavior,” in *Proc. 6th International Conference on Evolvable Systems-ICES 2005*, LNCS vol. 3637, pp. 108-118, 2005.

[13] S. L. Hooper, “Central pattern generators,” *Current Biology*, vol. 10, pp. R176-R177, 2000.

[14] P. Manoonpong, F. Pasemann, J. Fischer, and H. Roth, “Neural processing of auditory signals and modular neural control for sound tropism of walking machines,” *International Journal of Advanced Robotic Systems (ARS)*, vol. 2, no. 3, pp. 223-234.